Tables

Table 1: Petrographic characteristics of meteorites

Meteorite	Group	Matrix		Chondrules			Weathering	Fayalite		Ferrosilite (low-Ca Px)		Wollastonite	Plagioclase		Sulfides	Metal	Magnetite	Mag. Susc.	Ms	FeO in matrix (wt%)	Total in matrix (wt%)
		(vol%)	n	(vol%)	(µm)	n		(mol%)	n	(mol%)	n	(mol%)	(mol%)	n	(vol%)	(vol%)	(vol%)	(log χ) ($\times 10^{-9}$/kg)	(Am^2/kg)		
Chwichiya 002[a]	C3.00-ung	73.4*	421	12.9*	480±300	29	moderate	37.6±16.7	16	3.1±3.0	4	0.8±3	--	--	4.9*	<1.0*	7.8*	4.38*	3.29*	39.39	89.11
NWA 11750[b]	C3.00-ung	74.0	/	26.0	240±170	28	minimal	11.9±17.1	7	3.2±2.2	3	3.8±1.1	--	--	1.9**		--	4.03*	2.39*	34.30	96.45
NWA 12957[c]	C3.00-ung	63.3*	667	24.8	300±200	25	low	24.3±20.8	21	8.8±12.7	10	1.5±0.8	--	--	6.6*	1.0*	4.1*	4.44*	6.19*	31.86	81.86
EM 200[d]	C3	44.1*	669	35.2*	130±80	/	low	22.7±23.6	39	1.6±0.5	7	0.7±0.4	--	--	7.6*	<1.0*	10.7**	5.08*	17.10*	23.79	72.34

*: analyses from Krämer Ruggiu et al., 2021 (point counting); **: abundance calculated from M_S; --: not detected. Sulfides and metal abundances in NWA 11750 where not dissociated.-
Mag. Susc.: Magnetic Susceptibility; n: number of points for modal abundance, number of chondrules for chondrules sizes, or number of minerals for compositions; M_S: saturation magnetization.
Sulfides and metal in the matrix of NWA 11750 are finely intermixed, thus, we use saturation magnetization to get a bulk abundance of both sulfides and metal intermixed.
[a]: Gattacceca et al., 2021; [b]: Gattacceca et al., 2020b; [c]: Jacquet et al., 2016; [d]: Ruzicka et al., 2015

Table 2. Major (wt%) (ICP-OES) and trace element (ppm) (ICP-MS) bulk rock analyses.

	Chwichiya 002	NWA 11750	NWA 12957	EM 200
n	*3*	*3*	*3*	*3*
SiO_2	29.2	30.3	29.1	31.6
Al_2O_3	2.31	2.15	2.21	2.19
TiO_2	0.11	0.11	0.11	0.12
FeO	29.3	28.0	27.9	29.3
Cr_2O_3	0.49	0.48	0.46	0.49
MnO	0.19	0.21	0.21	0.19
MgO	19.1	20.6	18.5	21.8
CaO	4.06	6.29	4.10	1.60
Na_2O	0.36	0.20	0.39	0.18
K_2O	0.07	0.12	0.10	0.04
NiO	1.73	0.96	1.50	1.40
P_2O_5	0.31	0.34	0.28	0.25
Total*	87.2	89.9	84.9	89.1
RSD	1.23	0.86	1.31	5.91
Sc	10.95	8.90	9.12	9.82
V	104.0	99.2	92.1	103.7
Cr	3742	3602	3394	3791
Co	688	591	650	639
Ni	15515	8744	12945	12410
Cu	150.8	101.0	135.2	128.0
Zn	235.7	11.4	214.9	133.8
Rb	0.96	0.95	1.43	1.78
Sr	197.9	111.6	208.1	13.80
Y	2.82	2.89	2.84	2.46
Zr	8.24	8.87	10.50	8.50
Nb	0.31	0.33	0.36	0.35
Ba	516.1	383.5	419.5	16.5
La	1.02	0.78	1.36	0.64
Ce	1.65	1.39	2.16	1.25
Pr	0.20	0.19	0.30	0.15
Nd	1.20	1.09	1.49	0.99
Sm	0.28	0.33	0.40	0.29
Eu	0.10	0.11	0.12	0.09
Gd	0.41	0.45	0.45	0.37
Tb	0.07	0.08	0.07	0.06
Dy	0.56	0.53	0.49	0.42
Ho	0.10	0.11	0.10	0.09
Er	0.28	0.30	0.31	0.28
Tm	0.04	0.05	0.04	0.04
Yb	0.26	0.29	0.31	0.28
Lu	0.03	0.04	0.04	0.03
Hf	0.20	0.21	0.28	0.25
Pb	3.88	bdl	2.26	1.35
Th	0.08	0.11	0.15	0.11
U	0.70	0.17	0.50	0.01

Bdl: below detection limit; *: total without LOI; RSD: relative standard deviation; n: number of pieces measured for bulk analyses.

Table 3. XRD and PSD-XRD detections of different phases on bulk samples (vol%).

		Amorphous	Phyllosilicates	Carbonates	Pyrrhotite	Troilite	Magnetite	Metal	Olivine	Clino pyroxene	Ortho pyroxene
NWA 12957	XRD Section	x	--	3	5	--	x	--	44	16	8
	XRD Powder	x	--	5	2	--	x	1	48	21	x
	PSD-XRD	23	6	3	--	1	2	--	41	11	13
Chwichiya 002	XRD Powder	x	2	7	3	--	x	--	57	14	17
	PSD-XRD	12	5	1	--	3	4	--	45	6	24
NWA 11750	XRD Section	--	--	5	6	4	--	3	58	11	12
	XRD Powder	--	--	6	5	5	--	3	56	10	15
	PSD-XRD	--	2	2	2	1	--	1	63	15	14
EM 200	XRD Section	--	--	--	--	6	20	--	31	26	17
	PSD-XRD	--	2	--	1	--	16	--	39	18	24

"--" not detected; "x" means the phase was observed on the XRD pattern, but its quantitative modal abundance could not be measured.

Table 4. Bulk TGA results with associated IR signatures. TGA results are the mass loss (wt%) for each meteorite. IR indicates the gas signature(s) observed for each temperature range.

		Water (0-200°C)	(Oxy)hydroxides organics (200-400°C)	Phyllosilicates, sulfide, organics (400-770°C)	Carbonates (770-900°C)	Total mass loss without water (200-900°C)
NWA 12957	TGA	3.58	2.96	4.85	0.79	8.61
	IR	-	CO_2	CO_2/CO	CO_2	/
NWA 11750	TGA	1.45	1.50	8.55	0.96	11.02
	IR	-	-	CO_2/CO/CH	CO	/
Chwichiya 002	TGA	4.47	3.24	6.81	0.98	11.03
	IR	-	-	CO_2/CO	CO	/
EM 200	TGA	2.05	13.43	7.56	5.68	26.67
	IR	-	CH	CO_2/CO/SO_2	CO	/

Table 5. Modal abundances (vol%) calculated from SEM-EDS and TEM-EDS maps in the matrix.

		Carbonate	TCI	Phyllo silicate	Fine-grained mix	GEMS-like	Pentlandite	Troilite /Pyrrhotite	Magnetite	Metal	Olivine	Pyroxene	Plagioclase	Porosity
NWA 12957	SEM	--	5.29	--	45.2	--	11.0	2.01	6.12	<1	19.9	1.91	--	4.73
Chwichiya 002	SEM	--	22.0	--	65.6	--	3.14	<1	3.03	<1	2.94	1.75	--	1.59
Chwichiya 002	TEM	--	27.2	--	--	38.9	4.03	<1	4.96	1.27	3.13	5.94	--	14.6
NWA 11750	SEM	3.66	--	4.71	66.2	--	<1	6.84	--	3.60	--	5.03	3.14	3.70
NWA 11750	TEM	32.6	--	8.49	--	--	--	0.63	--	2.75	41.4	13.8	--	--
EM 200	SEM	--	--	--	57.4	--	2.39	6.28	1.95	2.74	17.7	5.28	--	6.29
EM 200	TEM	--	<1	54.1	--	--	1.27	4.14	2.40	1.35	18.2	4.72	--	13.7

Table 6: Matrix defocused EMP analyses (wt%)

(wt %)	SiO_2	Al_2O_3	TiO_2	FeO	Cr_2O_3	MnO	MgO	CaO	Na_2O	K_2O	NiO	S	**Total**
EM 200	24.90	3.86	0.05	23.79	0.31	0.17	11.50	1.59	0.24	0.10	1.92	1.96	**72.34**
NWA 12950	26.11	2.63	0.07	31.86	0.40	0.17	11.45	2.04	0.49	0.14	2.12	2.35	**81.86**
NWA 11750	29.90	2.75	0.10	34.30	0.43	0.22	17.47	4.83	0.21	0.17	1.92	2.27	**96.45**
Chwichiya 002	25.79	2.71	0.08	39.39	0.60	0.20	13.75	1.99	0.59	0.11	2.14	1.76	**89.11**

Table 7. Summary of detection of primary and secondary phases

	SEM-FEG *(m)*	TEM *(m)*	IR transm *(m)*	XRD *(b)*	PSD-XRD *(b)*	TGA *(b)*
Carbonates	++ >100 nm	++ fib section	+/- ~ 6 wt%	++ ~ 2 vol%	++ ~ 1 vol%	+ ~ 1 wt %
Phyllosilicates	+/- >100 nm	++ fib section	+ ~ 2 vol%	++ ~ 5 vol%	++ ~ 1 vol%	x Mixed with sulfides and organics
TCI	- > 100 nm	++ fib section	- Mixed with phyllo	o Too small coherence domains	o Too small coherence domains	x Mixed with other phases
Sulfides II (Pyrrhotite/Pentlandite)	-/+ > 100 nm	++ fib section	/ /	+ Pyrrhotite-troilite mixing	+ Pyrrhotite-troilite mixing	x Mixed with phyllo and organics
Magnetite	++ > 100 nm	++ fib section	/ /	++ ~ 5 vol%	++ ~ 2 vol%	/ /
Sulfides I (troilite)	++ > 100 nm	++ fib section	/ /	+ Mixed with pyrrhotite	+ Mixed with pyrrhotite	x Mixed with phyllo and organics
Amorphous /GEMS-like	o > 100 nm	+++ fib section	/ /	x No abundance given	++ ~ 5 vol%	/ /
Metal	++ > 100 nm	++ fib section	/ /	++ ~ 1 vol%	++ ~ 1 vol%	/ /

"--" to "++" indicate level of efficiency of the detection of each instrument, for each secondary phase provided directly beneath efficiency level.

"x" is detection without any modal abundance information. "/" is no detection allowed by the instrument. "o" is below detection limit.

(m): matrix analyses. (b) bulk analyses. "IR transm": IR in transmission. "Phyllo": phyllosilicates

Table 8. Modal abundance (vol. %) of components in Chwichiya 002, EM 200, NWA 11750, NWA 12957, compared with other CMs.

	Sub-type	Matrix (vol%)	Metal (vol%)	Sulfides (vol%)	Major sulfides	Carbonates (vol%)	Phyllosilicates (vol%)	TCIs (vol%)	Magnetite (wt%)	References
Chwichiya 002		73.4	<1.0[α]	3.0[β]	po + pn	1[β]	5[β]	22*	3.6	This work
NWA 12957		63.3	1.0[α]	1.0[β]	po + pn	3[β]	6[β]	5.3*	4.5	This work
NWA 11750		74.0	3.0[α]	3.0[β]	tro ≈ po	2[β] -33**	2[β]	3.7*	No	This work
EM 200		44.1	<1.0[α]	1.0[β]	tro	No[β]	2[β]	No*	17	This work
Paris	2.7	55.0	1.2[α]	0.7*	po + pn	1-3*	Abundant*	12*	6.4	Hewins et al., 2014; Rubin, 2015
	2.9		~ 3			Rare or no	Rare or no	No	No	
Asuka 12169	3.0	53.4	2.3[α]	1.4[α]	tro > po+pn	Rare or no	Rare or no	No[α]	No[α]	Kimura et al., 2020
Asuka 12236	2.9	64.8	1.5[α]	1.1[α]	tro > po+pn	Rare or no	Rare	No[α]	No[α]	Kimura et al., 2020
Asuka 12085	2.8	57.7	1.2[α]	0.9[α]	tro > po+pn	Minor	Minor	Minor[α]	Rare[α]	Kimura et al., 2020

Tro: troilite; pn: pentlandite; po: pyrrhotite; No: none.
Magnetite calculated from magnetic saturation magnetization Ms.
Matrix modal abundance done with optical microscopy; [α]: XRD; [β]: PSD-XRD; *: SEM; **: TEM

Figures captions

Figure 1: SEM-BSE images of the four studied chondrites: a: Chwichiya 002 (C3.00-ung); b: NWA 11750 (C3.00-ung); c: NWA 12957 (C3.00-ung); d: EM 200 (C3). Chondrules and chondrule fragments (dark gray) and metallic Fe-Ni nodules and sulfides (white) are embedded in abundant fine-grained silicate matrix material (light gray for Chwichiya 002, NWA 11750 and NWA 12957; dark gray for EM 200 caused by a less iron-rich matrix). Several chondrules contain small blebs of metallic Fe-Ni. Scale and contrast parameters are identical for all images.

Figure 2: $\delta^{17}O$-$\delta^{18}O$ (‰) diagram in carbonates in NWA 11750. Blue star is bulk isotopic composition of NWA 11750. TFL: terrestrial fractionation line; PCM: primitive chondrule minerals (Ushikubo et al., 2012).

Figure 3: Raman parameters of the four studied meteorites (Chwichiya 002, EM 200, NWA 11750 and NWA 12957) compared to type 3 chondrites and CM chondrites (R1, R2, R3, from Quirico et al., 2018). R1 group corresponds to highly primitive with no structural modifications by heating; R3 group corresponds to slight structural modifications induced by a weak heating; and R2 group corresponds to strongly heated chondrites.

Figure 4: Plot of the standard deviation vs. the mean of the Cr_2O_3 content of ferroan olivine. Hollow symbols represent Cr_2O_3 with <10 number of analyses. The dashed orange line is added as a tentative trend for CM meteorites. NWA 11750 plot close to Colony, Y-81020, and Paris, three 3.0 chondrites. NWA 12957 and Chwichiya 002 plot closer to Acfer 094 showing less heating than Paris meteorite. EM 200 has a high standard deviation plotting far from other carbonaceous chondrites. Green curve is carbonaceous chondrites, blue curve is ordinary chondrites, both from Grossman and Brearley (2005); Paris data from Hewins et al., 2014. CM data are from: Ruzicka et al., 2015, 2017; Bouvier et al., 2017; Gattacceca et al., 2016, 2020a, 2020b, 2021.

Figure 5: CI-normalized (Lodders et al., 2009) lithophile element concentrations in the four studied chondrites compared to CM and CO carbonaceous chondrite groups (data from Braukmüller et al., 2008). Elements are arranged in the order of increasing volatility (Wood et al., 2019).

Figure 6: Visible-near-infrared (VISNIR) reflectance spectra of studied samples (solid line) compared to spectra from reference CM carbonaceous chondrites (dashed line). Spectra were normalized at 0.55 µm and then offset for clarity.

Figure 7: SEM-EDS maps of A: Chwichiya 002; B: EM 200; C: NWA 12957; D: NWA 11750. Color code is Fe(Red), Mg(Green), Si(Blue), S(Yellow), Ni(Pink) for Chwichiya 002, EM 200 and NWA 12957. Fe(Red), Mg(Green), Si(Blue), S(Yellow), Ca(Pink) for NWA 11750. Scale is identical for all images.

Figure 8: STEM HAADF images: A: Chwichiya 002; B: NWA 11750; C: EM 200. Mt: magnetite; Ol: olivine; Px: pyroxene; Phy: nanocrystals of phyllosilicates; M: metal; Pn: pentlandite; Tro: troilite; Ca: carbonates.

Figure 9: TEM-EDS maps of: A: Chwichiya 002; B: NWA 11750; C: EM 200. Color code Fe(Red), Mg(Green), Si(Blue), S(Yellow), Ni(Pink) for Chwichiya 002 and EM 200. Fe(Red), Mg(Green), Si(Blue), Ca(Yellow) for NWA 11750. Nanophyllo : nano phyllosilicates; OM : Organic matter.

Figure 10: A: Chwichiya 002: A-1: TEM image of an amorphous GEMS-like material with small inclusions of sulfide and metal, surrounded by small TCIs; blue circle is the location of the SAED pattern on A-3; A-2: TEM-EDS map corresponding to 1a, metal in purple, sulfide in pink, TCIs in bright green to orange, amorphous material in dark green; A-3: SAED pattern of the amorphous phase in the GEMS-like material showing characteristic diffuse rings. Selected area aperture is 200 nm in diameter. B: NWA 11750: B-1: HR-TEM image shows crystalline olivines with carbonate and phyllosilicate; B-2: HR-TEM image of serpentine with d spacing measuring at 0.7 nm; B-3: HR-TEM image of crystalline olivine and carbonate in the fine-grained matrix. C: EM 200: C-1: small TCIs formed by sulfide and cronstedtite inside matrix formed by nanophyllosilicates and organic matter (OM); C-2: TEM-EDS map corresponding to C-1. Sulf: sulfides, Cro: cronstedtite, Phyllo: nanophyllosilicate, Ca: carbonate, Ol: olivine, OM: organic matter, Tro: troilite, M: metal.

Figure 11: Defocused EMP totals (wt%) in the matrix of the four studied meteorites compared to main carbonaceous chondrites groups. Data from Mc Sween and Richardson 1977; Ebert et al., 2019; Gattacceca et al., 2021.

Figure 12: Transmitted infrared spectra (absorbance) of the four samples at 20°C and 250/300°C. Absorbance is shifted for clarity. No data for NWA 11750 at 20°C were measured. Ca: carbonate; Ol: olivine; Px: pyroxene; Phy: phyllosilicates.

Figures

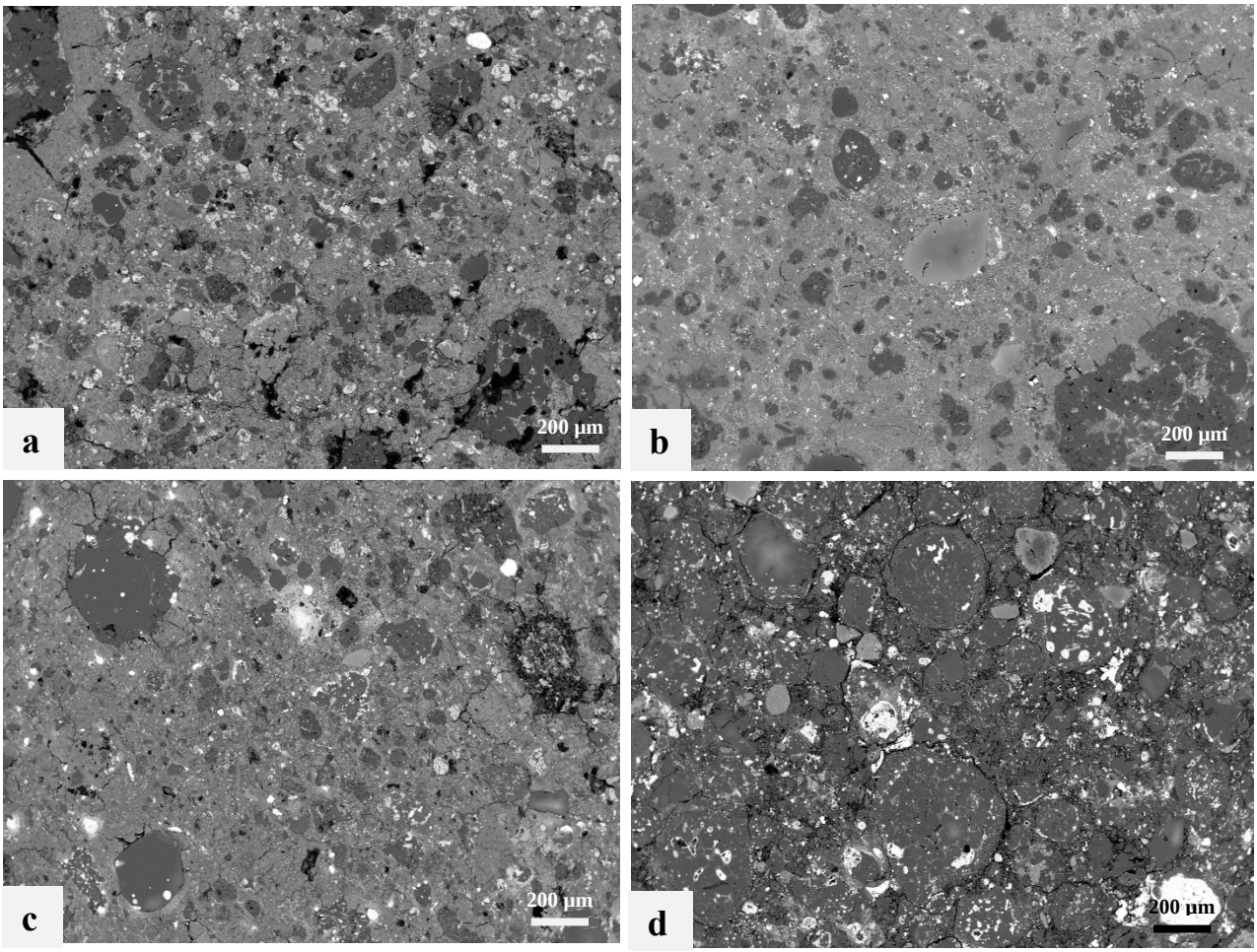

Figure 1: SEM-BSE images of the four studied chondrites: a: Chwichiya 002 (C3.00-ung); b: NWA 11750 (C3.00-ung); c: NWA 12957 (C3.00-ung); d: EM 200 (C3). Chondrules and chondrule fragments (dark gray) and metallic Fe-Ni nodules and sulfides (white) are embedded in abundant fine-grained silicate matrix material (light gray for Chwichiya 002, NWA 11750 and NWA 12957; dark gray for EM 200 caused by a less iron-rich matrix). Several chondrules contain small blebs of metallic Fe-Ni. Scale and contrast parameters are identical for all images.

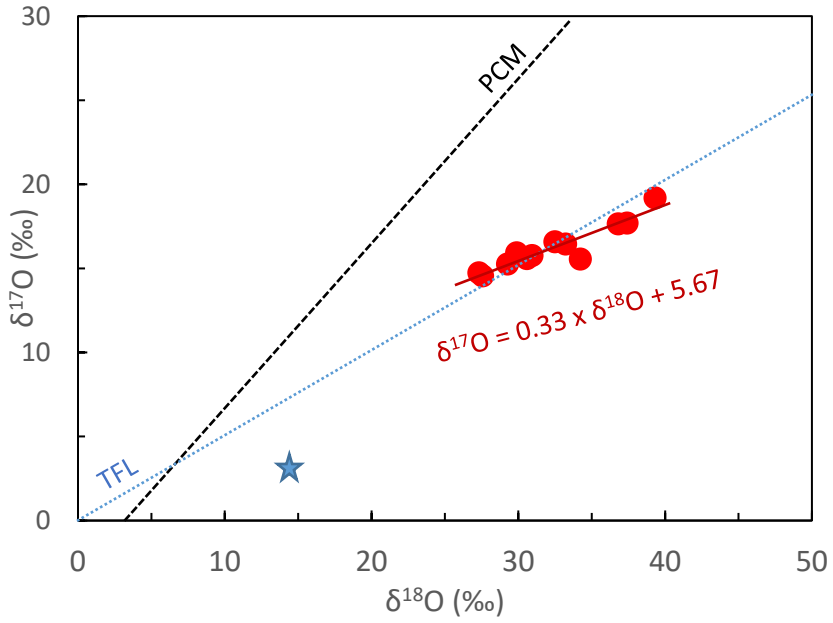

Figure 2: $\delta^{17}O$-$\delta^{18}O$ (‰) diagram in carbonates in NWA 11750. Blue star is bulk isotopic composition of NWA 11750. TFL: terrestrial fractionation line; PCM: primitive chondrule minerals (Ushikubo et al., 2012).

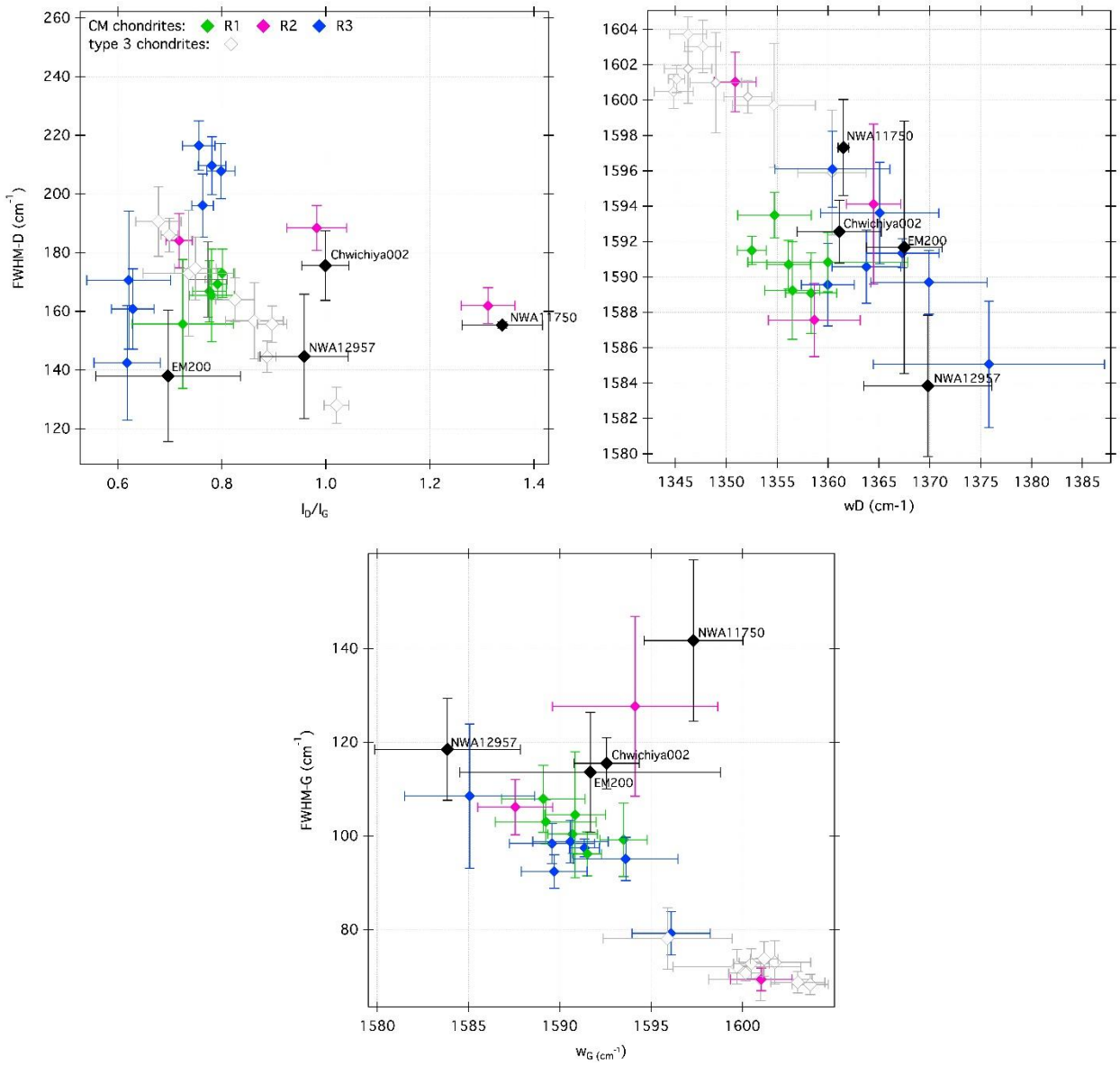

Figure 3: Raman parameters of the four studied meteorites (Chwichiya 002, EM 200, NWA 11750 and NWA 12957) compared to type 3 chondrites and CM chondrites (R1, R2, R3, from Quirico et al., 2018). R1 group corresponds to highly primitive with no structural modifications by heating; R3 group corresponds to slight structural modifications induced by a weak heating; and R2 group corresponds to strongly heated chondrites.

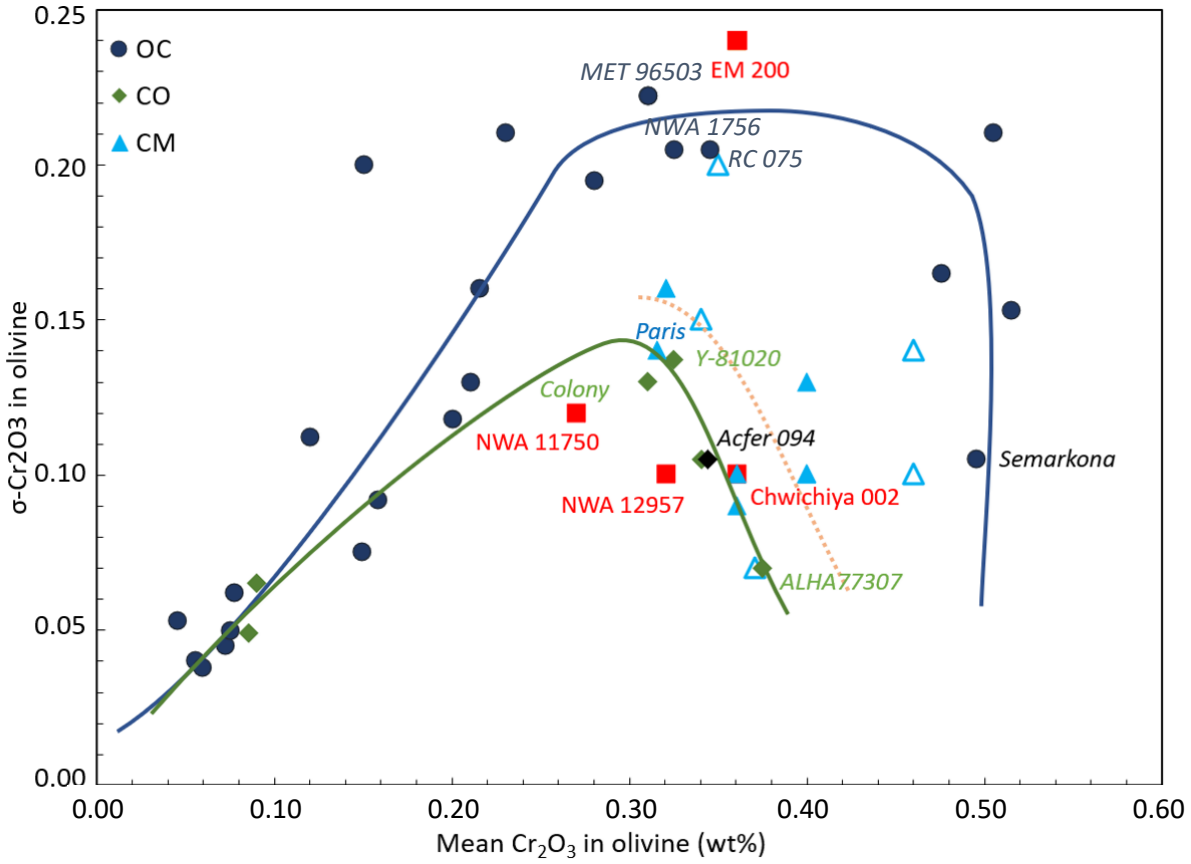

Figure 4: Plot of the standard deviation vs. the mean of the Cr_2O_3 content of ferroan olivine. Hollow symbols represent Cr_2O_3 with <10 number of analyses. The dashed orange line is added as a tentative trend for CM meteorites. NWA 11750 plot close to Colony, Y-81020, and Paris, three 3.0 chondrites. NWA 12957 and Chwichiya 002 plot closer to Acfer 094 showing less heating than Paris meteorite. EM 200 has a high standard deviation plotting far from other carbonaceous chondrites. Green curve is carbonaceous chondrites, blue curve is ordinary chondrites, both from Grossman and Brearley (2005); Paris data from Hewins et al., 2014. CM data are from: Ruzicka et al., 2015, 2017; Bouvier et al., 2017; Gattacceca et al., 2016, 2020a, 2020b, 2021.

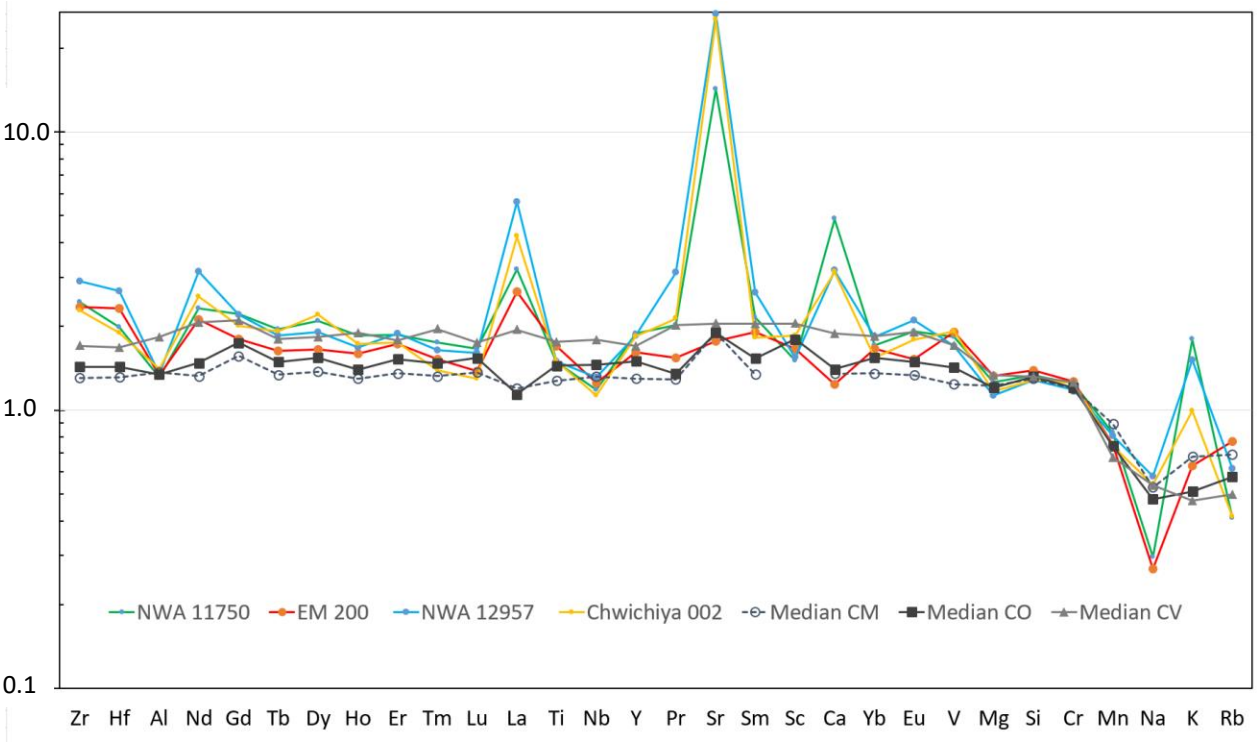

Figure 5: CI-normalized (Lodders et al., 2009) lithophile element concentrations in the four studied chondrites compared to CM and CO carbonaceous chondrite groups (data from Braukmüller et al., 2008). Elements are arranged in the order of increasing volatility (Wood et al., 2019).

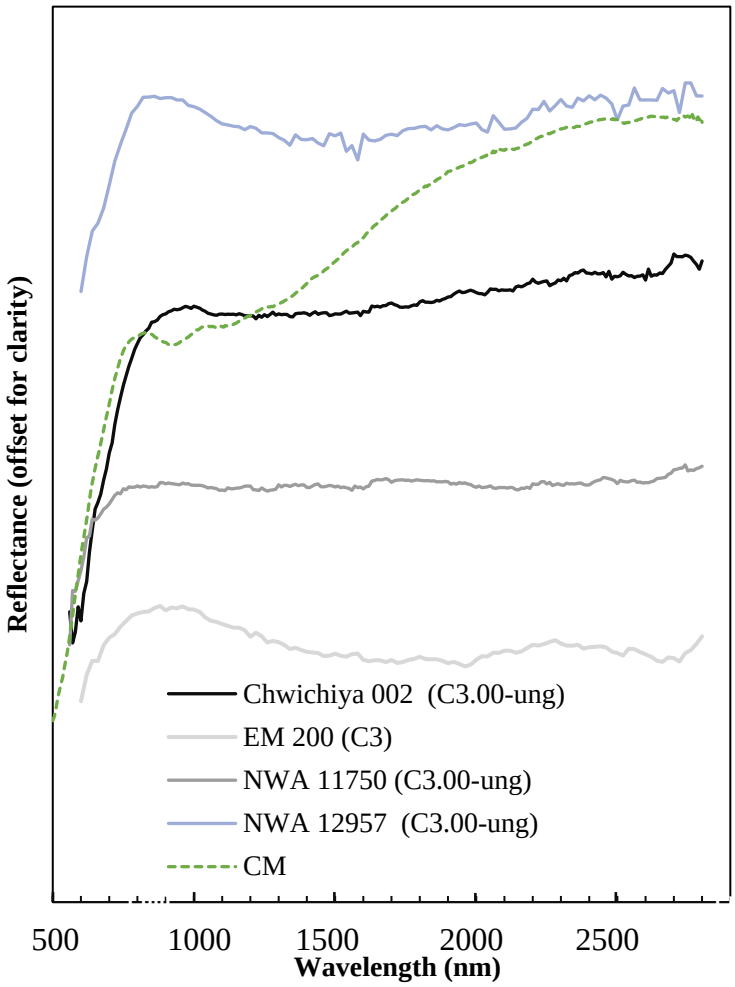

Figure 6: Visible-near-infrared (VISNIR) reflectance spectra of studied samples (solid line) compared to spectra from reference CM carbonaceous chondrites (dashed line). Spectra were normalized at 0.55 μm and then offset for clarity.

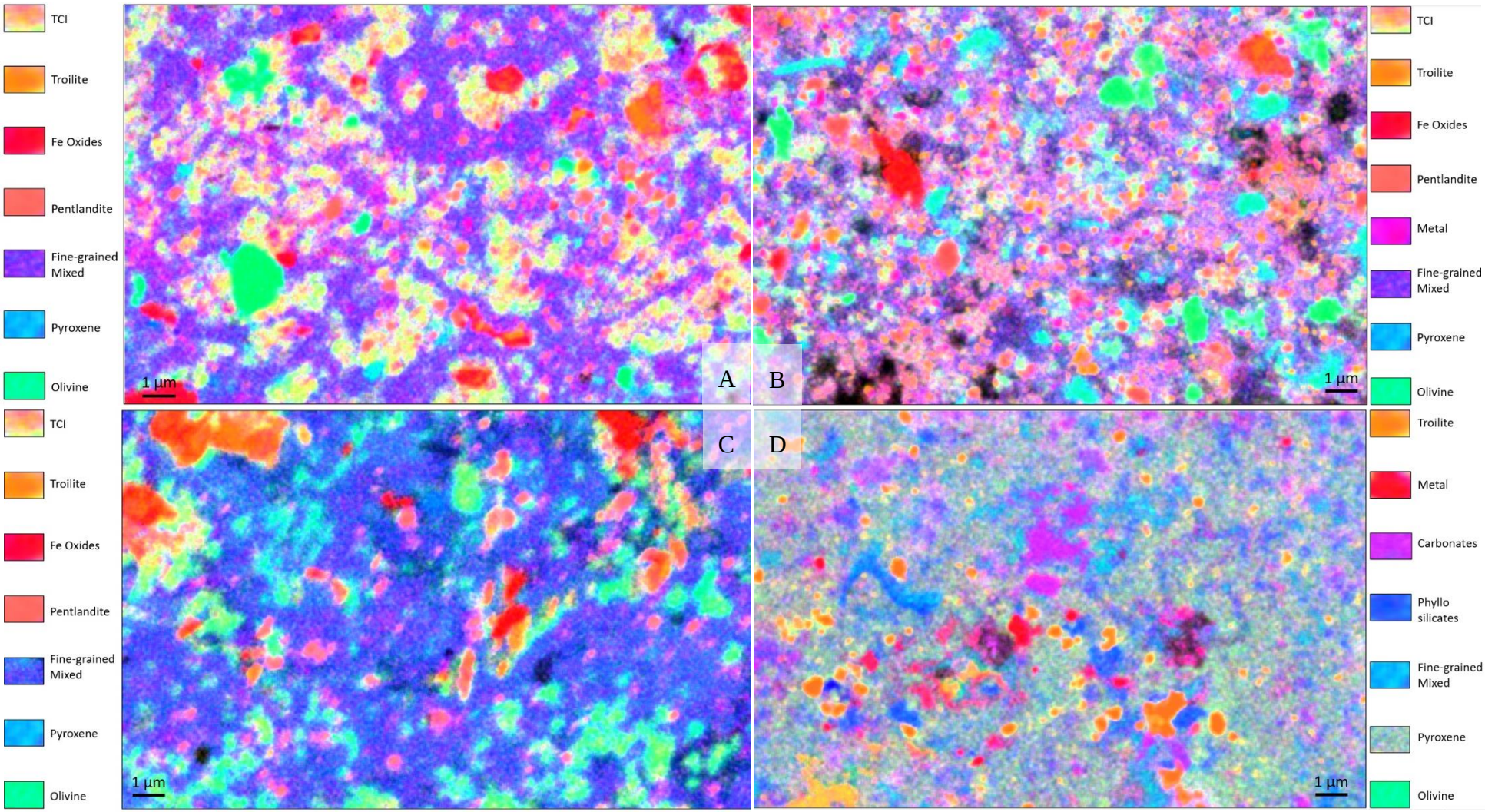

Figure 7: SEM-EDS maps of A: Chwichiya 002; B: EM 200; C: NWA 12957; D: NWA 11750. Color code is Fe(Red), Mg(Green), Si(Blue), S(Yellow), Ni(Pink) for Chwichiya 002, EM 200 and NWA 12957. Fe(Red), Mg(Green), Si(Blue), S(Yellow), Ca(Pink) for NWA 11750. Scale is identical for all images.

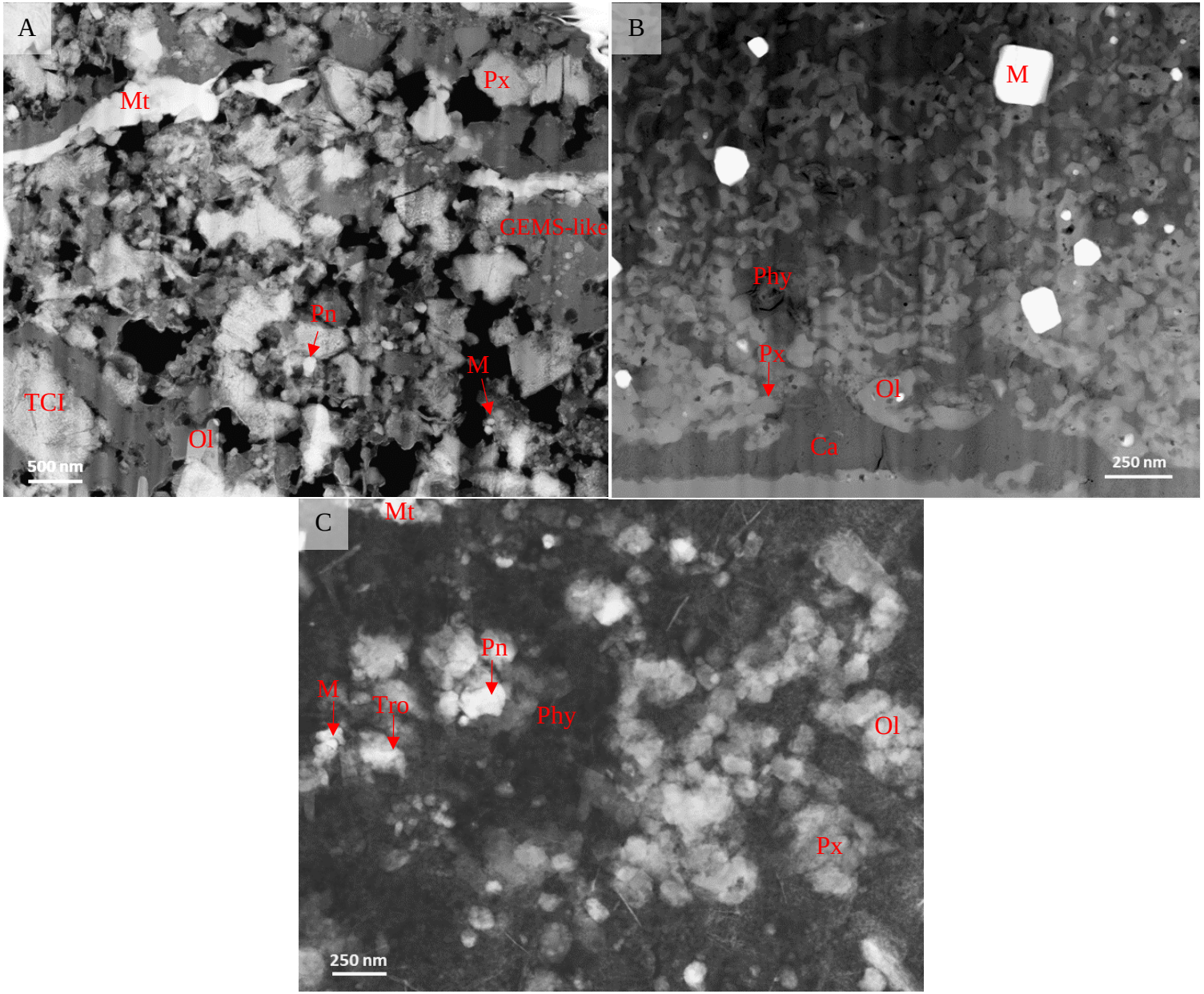

Figure 8: STEM HAADF images: A: Chwichiya 002; B: NWA 11750; C: EM 200. Mt: magnetite; Ol: olivine; Px: pyroxene; Phy: nanocrystals of phyllosilicates; M: metal; Pn: pentlandite; Tro: troilite; Ca: carbonates.

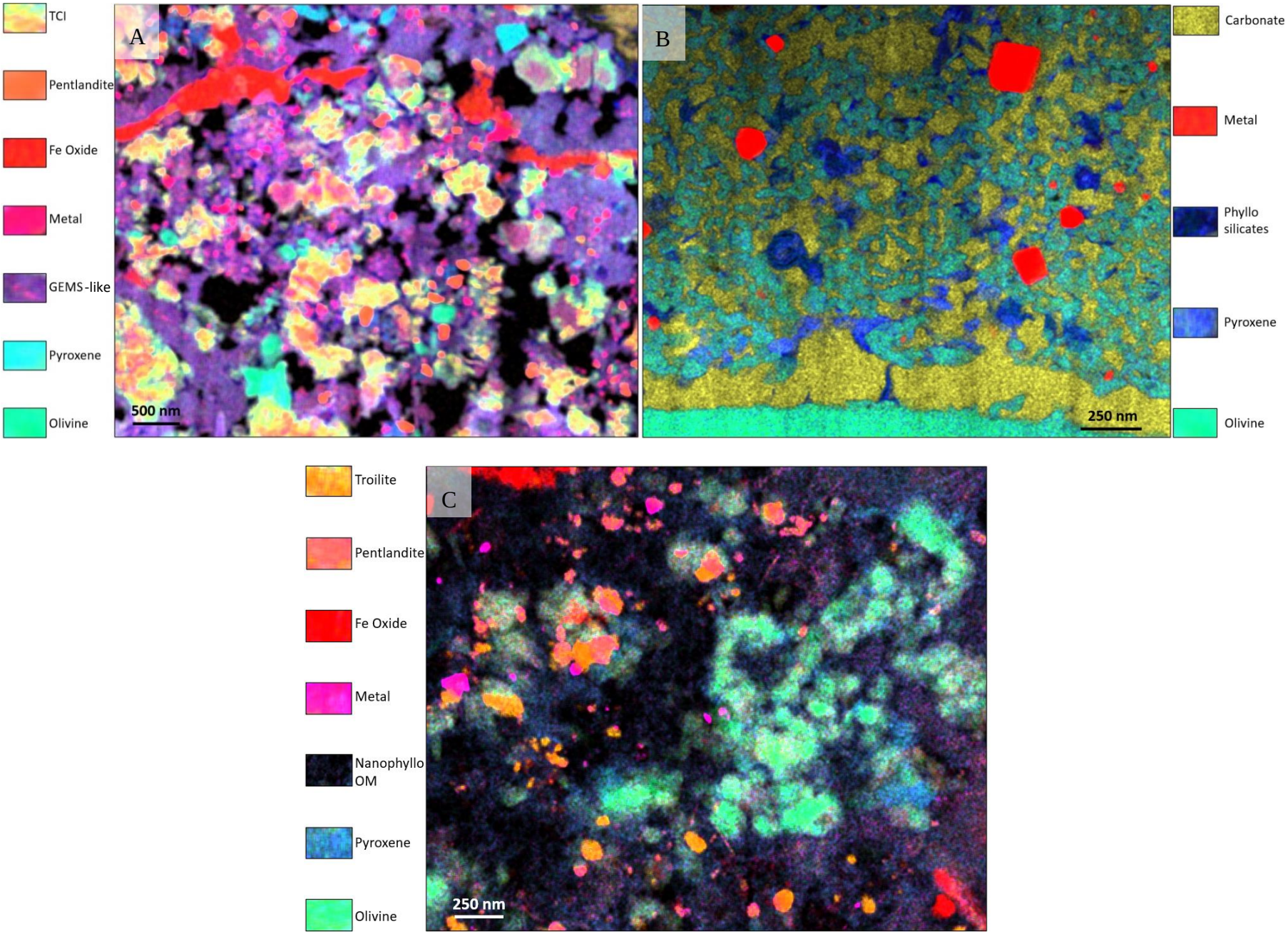

Figure 9: TEM-EDS maps of: A: Chwichiya 002; B: NWA 11750; C: EM 200. Color code Fe(Red), Mg(Green), Si(Blue), S(Yellow), Ni(Pink) for Chwichiya 002 and EM 200. Fe(Red), Mg(Green), Si(Blue), Ca(Yellow) for NWA 11750. Nanophyllo : nano phyllosilicates; OM : Organic matter.

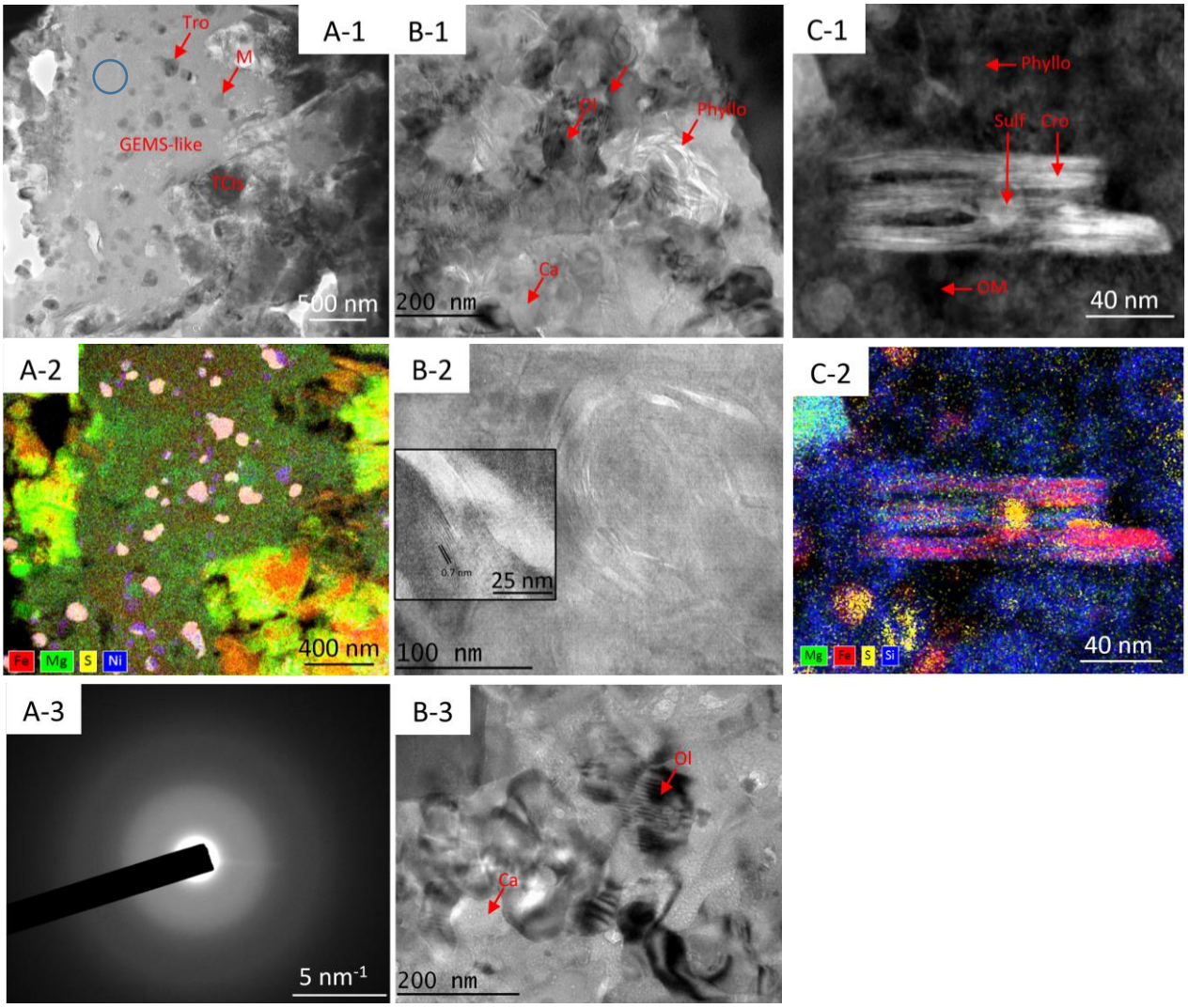

Figure 10: A: Chwichiya 002: A-1: TEM image of an amorphous GEMS-like material with small inclusions of sulfide and metal, surrounded by small TCIs; blue circle is the location of the SAED pattern on A-3; A-2: TEM-EDS map corresponding to 1a, metal in purple, sulfide in pink, TCIs in bright green to orange, amorphous material in dark green; A-3: SAED pattern of the amorphous phase in the GEMS-like material showing characteristic diffuse rings. Selected area aperture is 200 nm in diameter.

B: NWA 11750: B-1: HR-TEM image shows crystalline olivines with carbonate and phyllosilicate; B-2: HR-TEM image of serpentine with d spacing measuring at 0.7 nm; B-3: HR-TEM image of crystalline olivine and carbonate in the fine-grained matrix.

C: EM 200: C-1: small TCIs formed by sulfide and cronstedtite inside matrix formed by nanophyllosilicates and organic matter (OM); C-2: TEM-EDS map corresponding to C-1. Sulf: sulfides, Cro: cronstedtite, Phyllo: nanophyllosilicate, Ca: carbonate, Ol: olivine, OM: organic matter, Tro: troilite, M: metal.

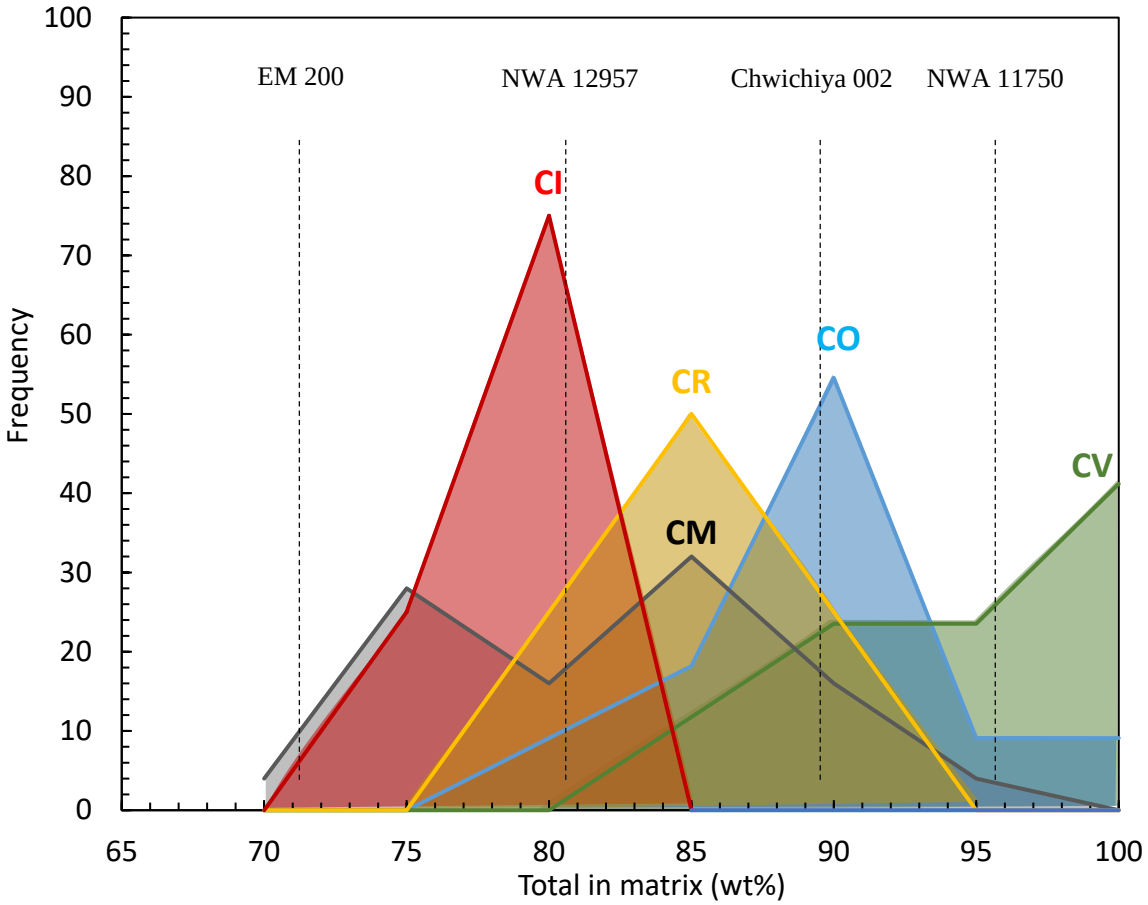

Figure 11: Defocused EMP totals (wt%) in the matrix of the four studied meteorites compared to main carbonaceous chondrites groups. Data from Mc Sween and Richardson 1977; Ebert et al., 2019; Gattacceca et al., 2021.

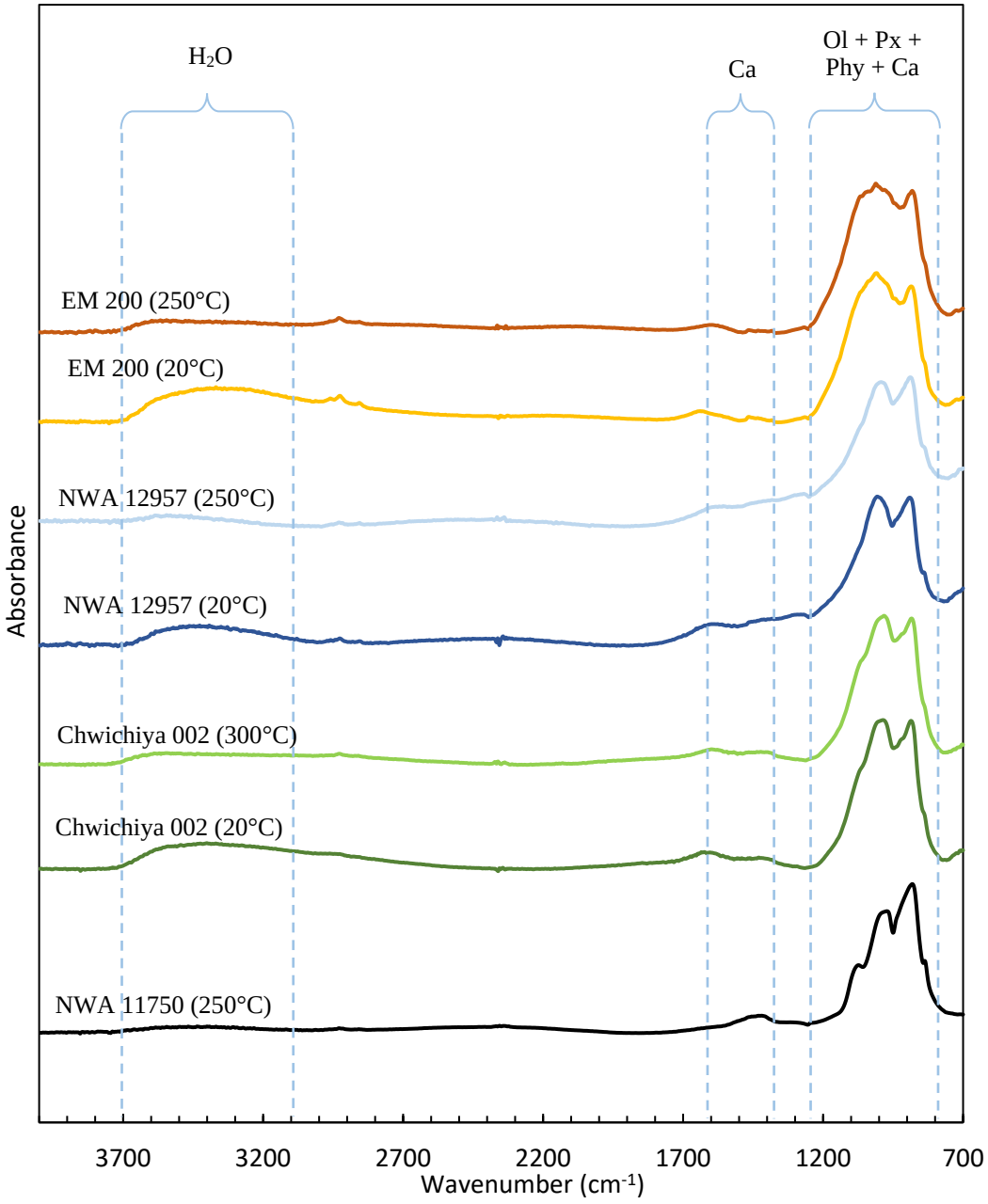

Figure 12: Transmitted infrared spectra (absorbance) of the four samples at 20°C and 250/300°C. Absorbance is shifted for clarity. No data for NWA 11750 at 20°C were measured. Ca: carbonate; Ol: olivine; Px: pyroxene; Phy: phyllosilicates.